Supporting Information

A doping of phosphorus and/or sulfur into nitrogen-doped carbon for efficient oxygen reduction reaction in acid media

Chang Hyuck Choi,[a] Min Wook Chung,[b] Sung Hyeon Park,[a] and Seong Ihl Woo*[,a,b]

[a]Department of Chemical and Biomolecular Engineering, [b]*Graduate* School of EEWS (WCU), Korea Advanced Institute of Science and Technology, Daejeon 305-701, Republic of Korea

*Corresponding author
Email: siwoo@kaist.ac.kr

Table of contents

1. Experimental procedures

1.1. Material preparations

Doped carbon materials were prepared by pyrolysis of a mixture composed of dicyandiamide (N- and C-precursor), metal chlorides (carbonization catalysts), and phosphoric acid (P-precursor) and/or cysteine (S-precursor). All chemicals used in the experiments were purchased from Aldrich. Specially, dicyandiamide (5 g), $CoCl_2$-$6H_2O$ (2.25 g), and $FeCl_2$-$4H_2O$ (0.75 g) were dissolved in distilled water (100 mL). For the additional doping of P and/or S, phosphoric acid (5 mmol) and/or cysteine (4 mmol) were added to the solution. The precursor solution was stirred for 1h, and the solvent was then evaporated under 300 mbar at 80 ^oC. The obtained gel-type mixture was further dried in an oven at 90 ^oC for 12 h. After cooling to room temperature, the mixture (5 g) was loaded on a quartz boat, and the boat was placed in a quartz tube in the furnace. The mixture was pyrolyzed at 900 ^oC for 3 h under an Ar atmosphere. Surface-exposed metal particles in the sample were removed by acid-leaching in 400 mL of aqua regia for 9 h. Finally, the sample was obtained after filtering, washing with distilled water (2 L), and drying in an oven.

1.2 Physical measurements

The transmission electron microscopy (TEM) images were taken at 200 kV with a JEM2100-F (Jeol Ltd.) equipped with an energy dispersive X-ray microanalysis (EDX). The X-ray diffraction (XRD) patterns were obtained by a D/MAX-2500 (Rigaku) operated at 40 kV and 300 mA. The step-scan patterns were collected in the 20^o to 80^o (2-theta ranges) with a step size of 0.01^o and a scan speed of 1^o min^{-1}. The Raman spectroscopy was performed using a LabRAM HR UV/Vis/NIR (Horiba Jobin Yvon) with a laser source of 514 nm. Compositions of the materials were examined by the element analysis (EA) using an EA1108 (CE instrument) and by the inductively coupled plasma (ICP) using a Poly Scan 6o E (Hewlett Packard). The XPS analysis was performed using a Sigma Probe (Thermo VG Scientific) equipped with a microfocused monochromator X-ray source. In the XPS results, peaks from dopants was deconvoluted by N1 (pyridinic-N, 398.6 eV), N2 (graphitic- or pyrrolic-N, 400~401 eV), and N3 (pyridinic-oxide, 403.5 eV) for N;[1] P1 (metal phosphide, 129.4 eV), P2 (P-O, 133.2 eV), and P3 (P-C, 134.8 eV) for P;[2] and S1 (-S-C-S-, 163.8 eV), and S2 (-C-$S(O)_x$-C-, 167.7 eV) for S.[3]

1.3 Electrochemical measurements

---

[1] U. S. Ozkan, P. H. Matter, L. Zhang, *J. Catal.* 2006, **239**, 83.
[2] C. H. Choi, S. H. Park, S. I. Woo, *ACS nano* 2012, **6**, 7084.
[3] C. H. Choi, S. H. Park, S. I. Woo, *Green Chem.* 2011, **13**, 406.

The electrochemical properties of the catalysts were characterized using a CHI700D (CH Instruments Inc.) and a RRDE-3A (ALS Co.) in a three-electrode beaker cell equipped with a Pt wire counter electrode (ALS Co., 002233), an Ag/AgCl reference electrode (ALS Co., 012167), and a ring disk electrode (ALS Co., 011169). The catalysts (10 mg) were dispersed in a Nafion ink solution, then the ink (5 μL) was dropped onto the glassy carbon (3 mm) of the ring disk electrode. The inks were dried at room temperature. The linear sweep voltammetry (LSV) was performed in 1M $HClO_4$ electrolyte purged with nitrogen or oxygen over 1h, with a 15 mV s^{-1} scan rate from 0.82 to -0.08 V (*vs.* Ag/AgCl). The ORR currents were obtained by subtracting the LSV results in an oxygen-saturated electrolyte by the results from the nitrogen-purged electrolyte, in order to remove the capacitance of the catalysts. A Tafel plot was obtained from the following equation:

$$1/I = 1/I_k + 1/I_d$$

Here, I_k is the kinetic current, and I_d is the diffusion limiting current. All mass activities were calculated through kinetic currents divided by the unit mass of the catalyst. The H_2O_2 formation yield was derived from the current at the Pt ring disk electrode. A constant potential (1.0 V, *vs.* Ag/AgCl) was applied to the Pt ring disk electrode during the ORR experiment and a 0.37 of collection efficiency was used. All potentials shown in this paper were converted to the reversible hydrogen electrode (RHE) scale. The current-time chronoamperometric was obtained at 0.38 V (*vs.* Ag/AgCl) for 10 h in 1M $HClO_4$ with continuous oxygen bubbling and commercial Pt/C (40 wt. %, E-tek) was used for comparison. The accelerated degradation test (ADT) was performed by the 5000^{th} potential cycling from 0.38 to 0.78 V (*vs.* Ag/AgCl) with 100 mV s^{-1} scan rate in 1M $HClO_4$.

2. Figures and Tables

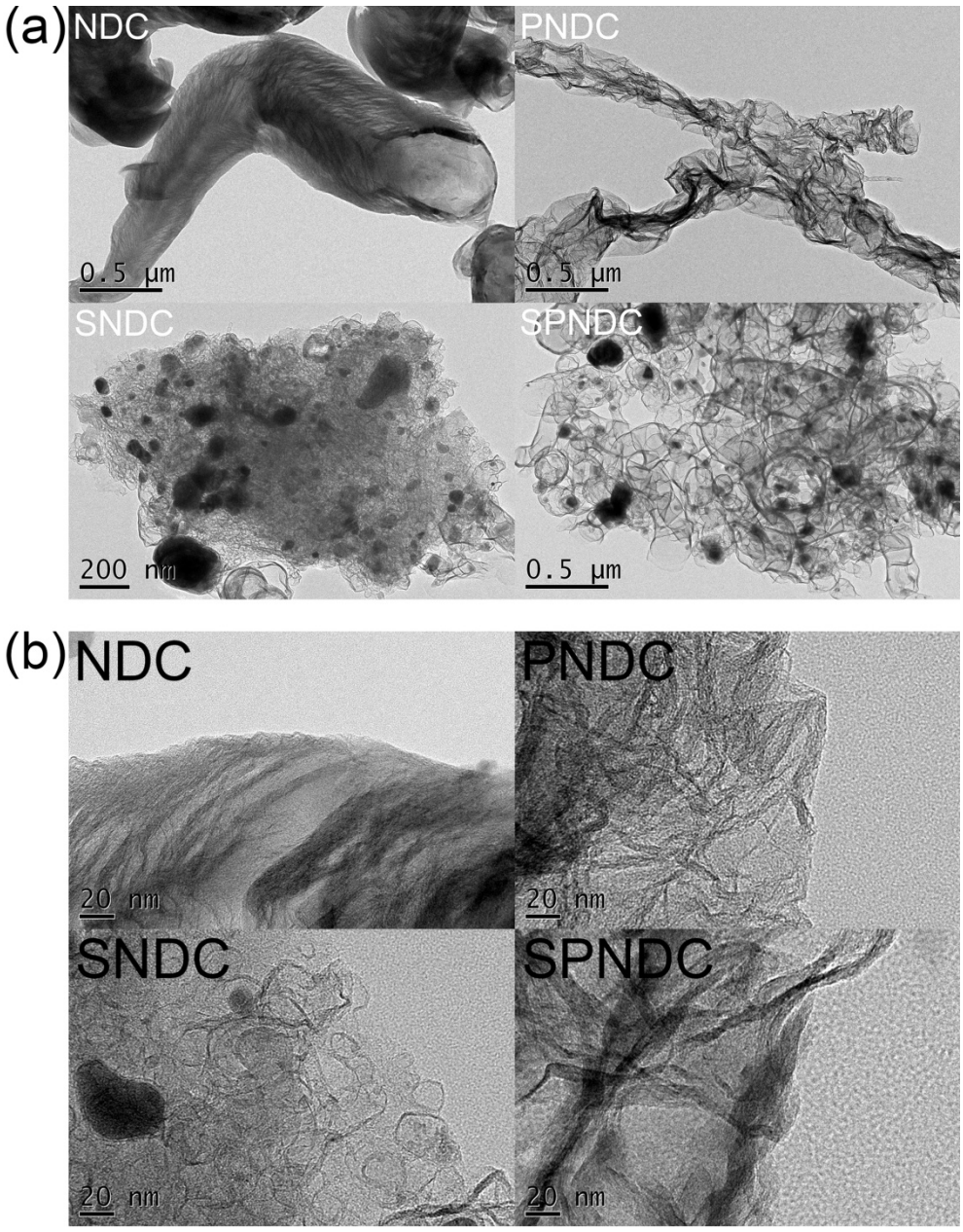

Figure S1. TEM images of the prepared carbon materials under (a) low and (b) high magnification.

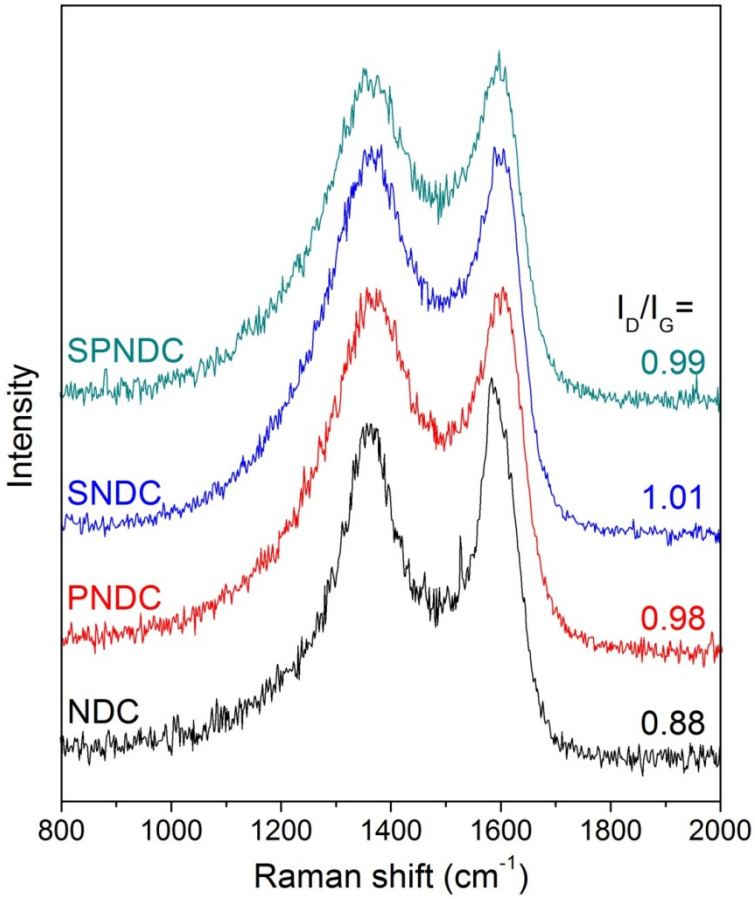

Figure S2. Raman spectroscopies of the prepared carbon materials. Intensity ratios of D- to G-band (I_D/I_G) are denoted in the figure.

In the Raman spectroscopy of all sp^2-carbon, two conspicuous peaks emerged, at around 1580 cm^{-1} of the G-band and 1352 cm^{-1} of the D-band. The G-band arises from the E_{2g} vibrational mode in the D_4^{6h} symmetry group of graphite crystal planes and is seen for all sp^2-carbon.[4] The D-band originates from lattice distortion in sp^2-hybridized carbon and is affected by the presence of various defects (*e.g.* vacancies, topological defects, and impurities). The ratio of the D- and G-band intensities (I_D/I_G) is generally used as a measure of the degree of carbon disorder. As shown in Figure S2, NDC reveals 0.88 of I_D/I_G value, whereas those of the additionally P- and/or S-doped carbons show higher values (~1 of I_D/I_G values). This shows that the additional doping of P and/or S produces many defect sites and derives lattice distortion in carbon materials.

[4] Y. Wang, D. C. Alsmeyer, R. L. Mccreery, *Chem. Mater.* 1990, **2**, 557.

Table S1. Compositions of the prepared carbon materials obtained by element analysis (EA) and inductively coupled plasma (ICP).

Catalysts	N[1]	C[1]	H[1]	S[1]	P[2]	Co[2]	Fe[2]
NDC	3.92	88.52	0.33	-	-	2.14	1.10
PNDC	5.37	78.25	0.40	-	1.06	6.47	2.48
SNDC	7.58	58.14	0.44	0.57	-	18.85	6.56
SPNDC	6.66	51.94	0.65	1.38	5.98	18.43	6.62

[1]Obtained from EA (wt. %), [2]Obtained from ICP (wt. %)

The compositions of the prepared carbon materials were obtained by EA and ICP methods. The EA analysis indicates that the dopants (*i.e.* N, S, and P) are effectively doped in the carbon materials. In spite of the iterative acid treatment with aqua regia, the carbon materials have metal residues with amounts that increased as additional heteroatoms were doped. The sum of the compositions is not 100 wt. % because some elements (*e.g.* oxygen) in the carbon cannot be analyzed by EA and ICP.

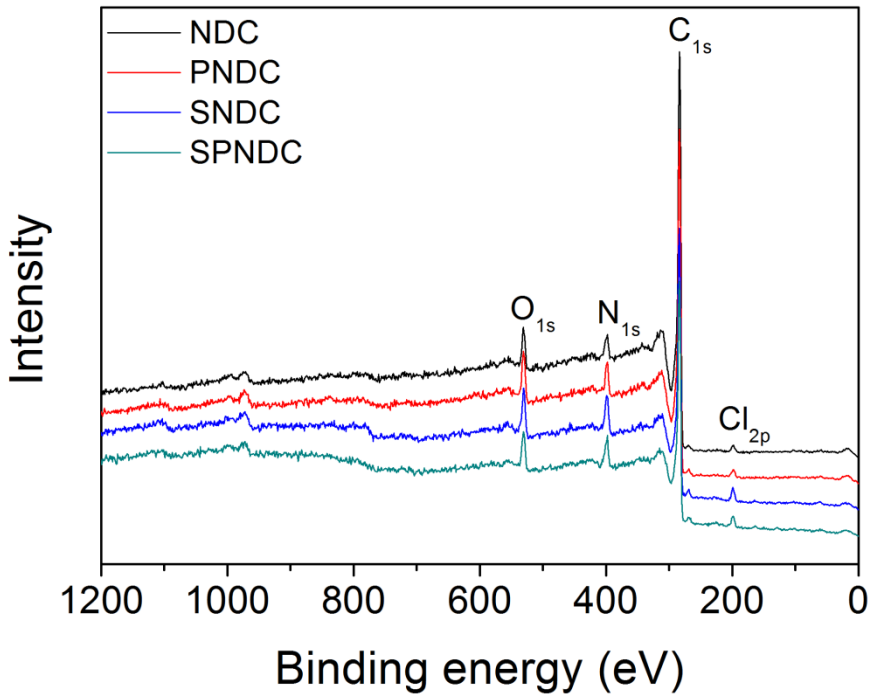

Figure S3. Full XPS survey scans of the prepared carbon materials.

At the surface of the prepared catalysts, carbon and oxygen are dominant elements, and some oxygen and chlorine are also detected due to the surface functional groups produced by the acid-leaching step.

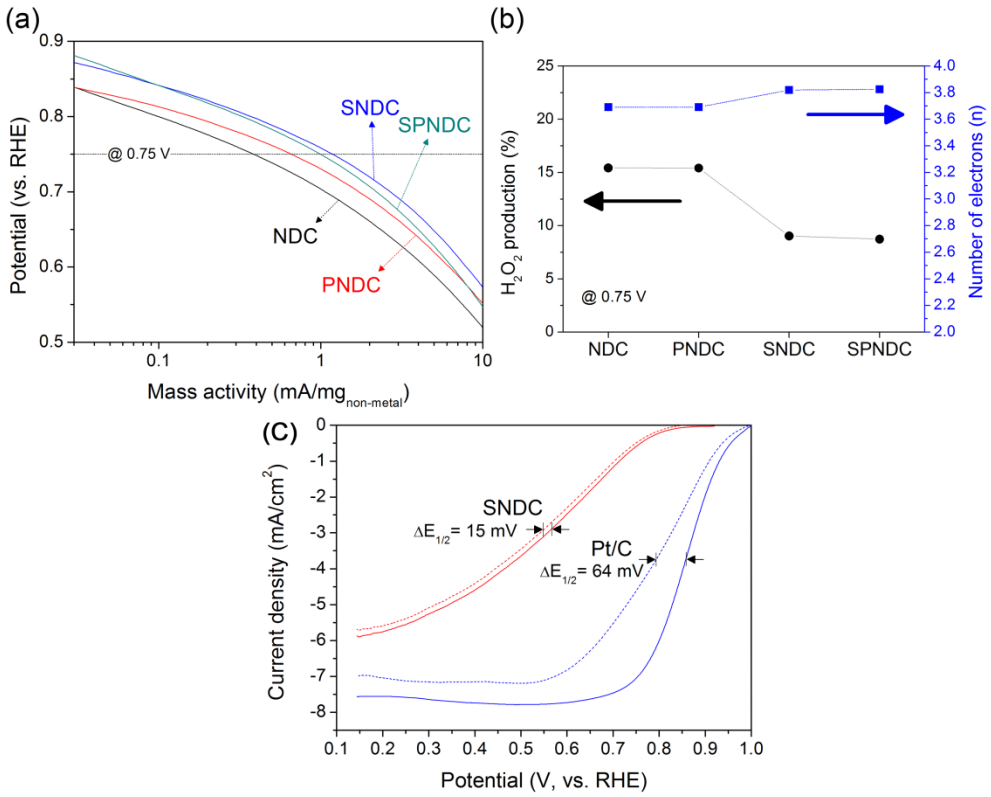

Figure S4. (a) Tafel plots of the prepared catalysts based on the unit mass of the non-metal parts, and (b) H_2O_2 production yields and number of transferred electrons at 0.75 V (*vs.* RHE) calculated from the Pt-ring disk electrode during the ORRs. (c) LSV results of SNDC and Pt/C in oxygen-bubbled 1M $HClO_4$ before (dotted line) and after (solid line) the 5000th potential cycling between 0.6 and 1.0 V (*vs.* RHE).

In Figure S4a, the Tafel plots based on the unit mass of the non-metal parts were calculated *via* the normalization of the kinetic currents in the ORRs by dividing the unit mass of the non-metal parts, in this case C, N, H, P, and S (from Table S1). As shown in Table S1, these carbon materials have considerable amounts of metal residues which are covered by carbon shells. Therefore, normalization by non-metal parts is meaningful to compare the mass activity without metal residues, which cannot participate in the ORRs due to carbon-encapsulation. From the results, the mass activities normalized by the non-metal parts of the prepared catalysts are 0.38, 0.66, 1.18, and 0.99 $mA/mg_{non\text{-}metal}$ for NDC, PNDC, SNDC, and SPNDC, respectively.

The ORR pathways were investigated by the RRDE technique, and the results are shown in Figure S4b. The catalysts shows 15.4, 15.4, 9.0, and 8.7 % of H_2O_2 production yields in ORRs at 0.75 V, and corresponding to 3.70, 3.70, 3.82, and 3.83 electron pathways for NDC, PNDC, SNDC, and SPNDC, respectively. Therefore, it can be concluded that additional doping of S in the NDC is favorable for the four-electron pathway, which produces H_2O.

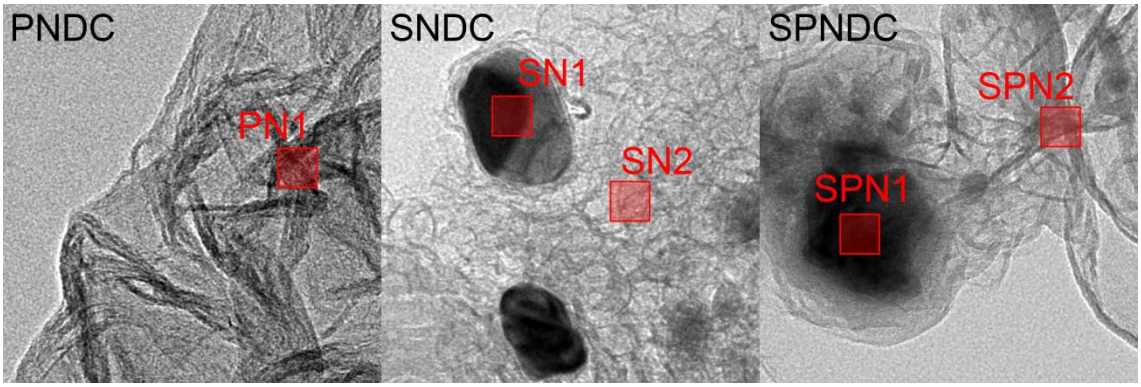

Figure S5. TEM images of PNDC, SNDC, and SPNDC. Red rectangles indicate the areas where EDX analysis is performed.

Table S2. Compositions of PNDC, SNDC, and SPNDC at selected points in Figure S5 by EDX analysis.

Catalysts	PNDC[1]	SNDC[1]		SPNDC[1]	
Points	PN1	SN1	SN2	SPN1	SPN2
C	93.5	82.6	92.3	71.2	92.3
N	6.5	5.8	7.4	5.9	6.6
P	-	-	-	6.2	0.4
S	-	0.1	0.3	0.3	0.7
Co	-	8.3	-	12.4	-
Fe	-	3.2	-	34.0	-

[1] at. %, error range is ±0.5 at. %.

[Notice] EDX is a very convenient technique for composition analyses. However, in the case of light elements (*e.g.* N, S, or P), reliable results cannot be obtained due to the low intensity and the overlapping of signals. Therefore, these results (Table S2) are not accurate compositions of the selected regions and do not represent the compositions of the carbon materials. These results are only used to investigate the doping sites of heteroatoms by comparing the EDX signals from metal and carbon.

As shown in Table S2, P is not detected on the carbon region in PNDC (the PN1 site in Figure S5). Similarly, P on the carbon region in SPNDC (SPN2 site) indicates low P signals (0.4 %). However, the metal region in SPNDC (SPN1 site) discloses much higher signals of P (6.2 %). The XRD results confirm that this phase is metal phosphide (Figure 1b). Therefore, P is dominantly bonded with the metals, and only small quantities of P (under the XPS detection limit (< 1 at. %)) are doped in the carbon lattice.

On the other hand, S is dominantly doped in the carbon lattice. Table S2 indicates higher signals of S in the carbon region (SN2 in SNDC and SPN2 in SPNDC) than those in the metal region (SN1 in SNDC and SPN2 in SPNDC). It is assumed that the low intensity of the S signals is detected in the metal region because the metal is covered by the carbon-shells, which are doped by S.

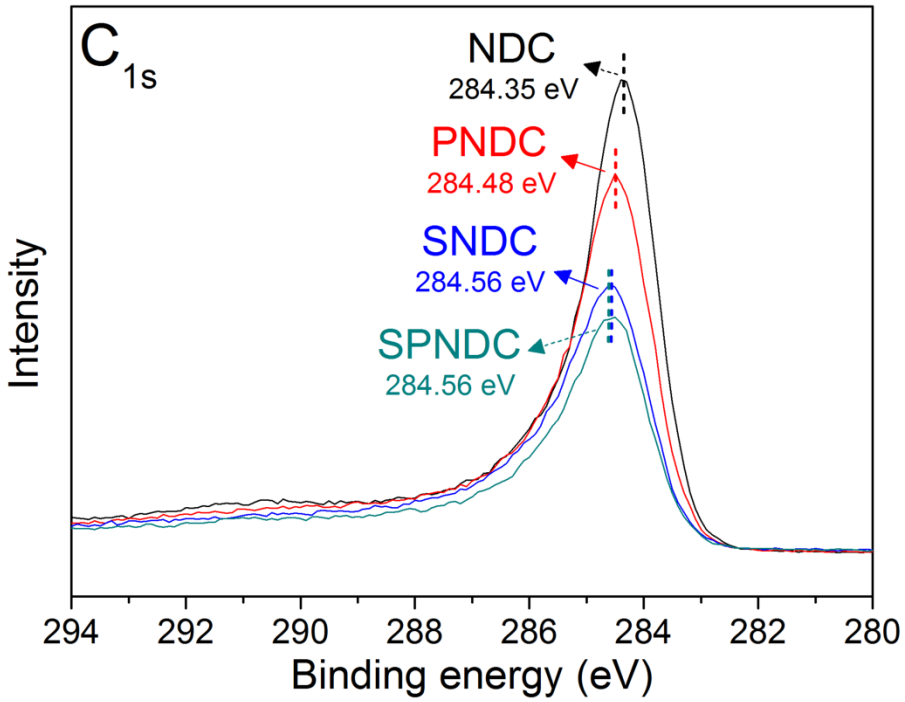

Figure S6. XPS-C_{1s} results of the prepared carbon materials.